Differential Analysis of Human Leukocytes by Dielectrophoretic Field-Flow-Fractionation

Jun Yang, Ying Huang,* Xiao-Bo Wang, Frederick F. Becker, and Peter R. C. Gascoyne
Department of Molecular Pathology, The University of Texas M. D. Anderson Cancer Center, Houston, Texas 77030, USA

ABSTRACT The differential analysis of human leukocytes has many important biological and medical applications. In this work, dielectrophoretic field-flow-fractionation (DEP-FFF), a cell-separation technique that exploits the differences in the density and dielectric properties of cells, was used to separate the mixtures of the major human leukocyte subpopulations (T- and B-lymphocytes, monocytes, and granulocytes). The separation was conducted in a thin chamber equipped with an array of microfabricated interdigitated electrodes on the bottom surface, and the separation performance was characterized by on-line flow cytometry. To investigate optimal separation conditions for different leukocyte mixtures, elution fractograms at various DEP field frequencies were obtained for each leukocyte subtype. With appropriately chosen conditions, high separation performance was achieved in separating T- (or B-) lymphocytes from monocytes, T- (or B-) lymphocytes from granulocytes, and monocytes from granulocytes. DEP-FFF does not involve cell-labeling or cell-modification step, and provides a new approach to hematological analysis.

INTRODUCTION

The enumeration and purification of human leukocyte subpopulations is fundamental in many biological and medical applications. For example, highly purified cells are required for analyses of functional capacities of the different leukocytes in immune responses, for studies of interleukin-mediated molecular signaling between leukocyte subpopulations (Trinchieri et al., 1992; Stout, 1993), and for characterization of leukocyte growth factors (Cantrell et al., 1992) and cytokines (Stein and Dalgleish, 1994; Couraud, 1994). Differential analysis of human leukocytes is routinely performed in clinical laboratories to identify leukemia and to discriminate between bacterial and virus infections. Methods currently used to discriminate and separate leukocyte subpopulations exploit cell properties such as density (Boyum, 1974; Ali, 1986), electrostatic characteristics (Gadeberg et al., 1979; Eggleton et al., 1992), and specific immunologic receptor–ligand interactions (Barald, 1987; Chess and Schlossman, 1976; Smeland, 1992; Miltenyi et al., 1990; Abts et al., 1989; Semple et al., 1993; NRC report, 1987). The techniques most widely used are rosetting (Barald, 1987), fluorescence-activated cell sorting (van Zaanen et al., 1995), and magnetic-activated cell sorting (Smeland, 1992; Miltenyi et al., 1990; Abts et al., 1989; Semple et al., 1993). The major disadvantages of these techniques are that cell labeling is time consuming and may interfere with cell use after separation. In addition, these methods cannot be readily implemented on simple, automated, portable diagnostic devices. Therefore, improved cell sorting methods that can identify and selectively manipulate different cell types based on novel physical properties are desirable.

Dielectrophoresis (DEP) is the movement of particles in a nonuniform AC electrical field driven by forces arising from the interaction between the field-induced polarization and the applied field (Pohl, 1978). It is currently being exploited for potential applications in cell separation. DEP separation is based on the principle that the polarizability of living cells depends strongly on their composition, morphology, and phenotype and on the frequency of the applied electrical field (Huang et al., 1996; Fuhr and Hagedorn, 1996; Pethig and Kell, 1987). Thus, cells of different types and in different physiological states have been found to possess distinctly different dielectric properties that can, under appropriate conditions, give rise to differential DEP forces and be exploited for cell separation (Gascoyne et al., 1992, 1997; Wang et al., 1993; Markx et al., 1994, 1995; Becker et al., 1994, 1995; Stephens et al., 1996; Cheng et al., 1998a,b).

A recently developed technique, DEP field-flow-fractionation (DEP-FFF), exploits the balance of DEP levitation and gravitation forces. Cells having different density and dielectric properties are levitated to different heights above the bottom surface of a thin chamber, and are carried with the fluid flow at different velocities when a parabolic flow velocity profile is generated inside the chamber (Fig. 1). Like most chromatographic methods, DEP-FFF operates in a batch-mode, so the separated cells are eluted from the chamber at different times. DEP-FFF has been used to separate human leukemia (HL-60) cells from normal human mononuclear cells (Huang et al., 1997), synthetic polystyrene microbeads of different sizes and different surface functionalization (Wang et al., 1998), and human breast cancer (MDA-

Received for publication 6 August 1999 and in final form 24 January 2000.

Address reprint requests to Dr. Jun Yang, University of Texas M. D. Anderson Cancer Center, Department of Molecular Pathology, Box 89, 1515 Holcombe Blvd., Houston, TX 77030. Tel.: 713-792-7605; Fax: 713-792-5940; E-mail: turnip@solace.mdacc.tmc.edu.

Dr. Huang's present address is Nanogen, Inc., 10398 Pacific Center Ct., San Diego, CA 92121.

Dr. Wang's present address is Artloon Corp., 3985A Sorrento Valley Blvd., San Diego, CA 92121.

© 2000 by the Biophysical Society

0006-3495/00/05/2680/10 $2.00

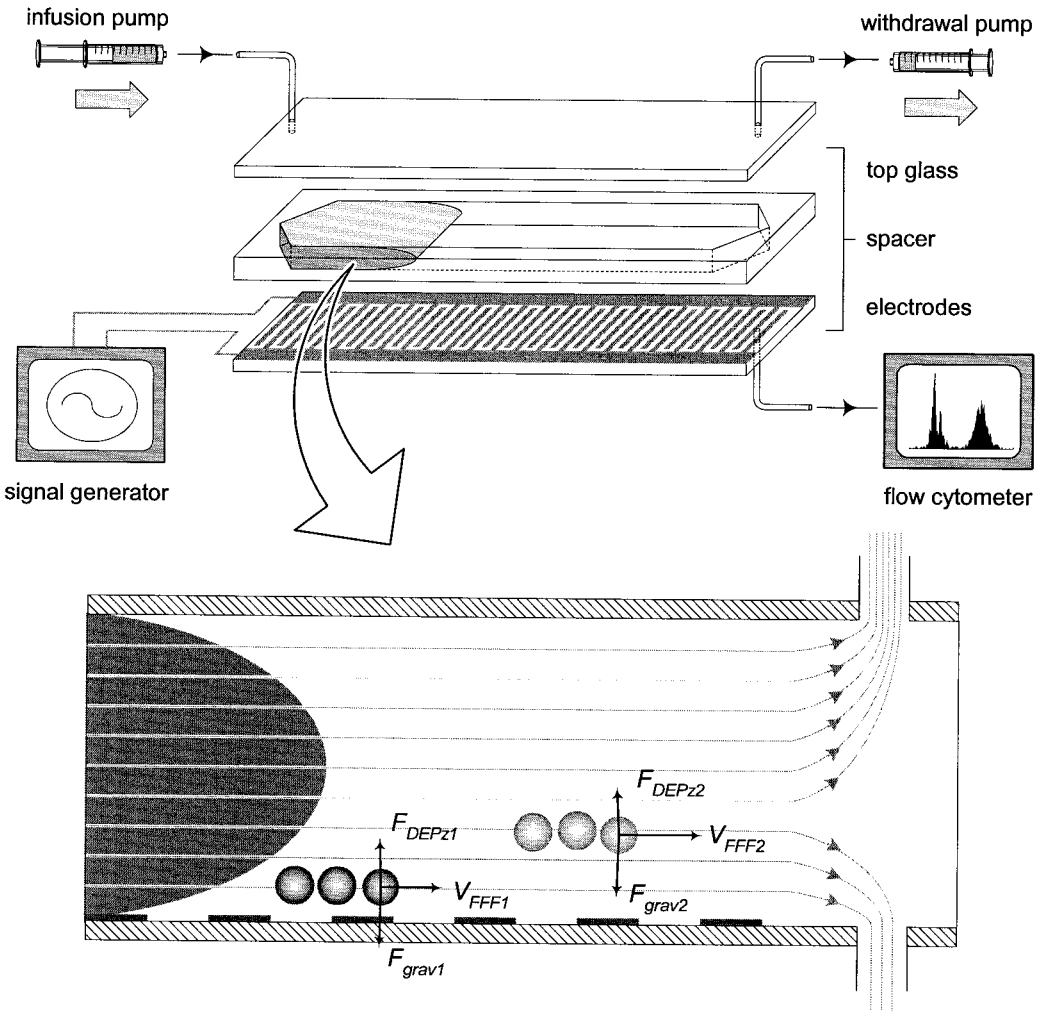

FIGURE 1 DEP-FFF principle and system setup. DEP-FFF chamber was constructed with microfabricated, interdigitated electrode arrays on its bottom wall. Cells having different dielectric properties are levitated to different heights within a fluid-flow velocity profile inside a thin chamber and are carried with the fluid flow at different velocities. In this configuration, the cells exit the chamber through the outlet port on the chamber bottom, and the majority of the cell-free carrier medium is eluted through the top outlet port.

435) cells from whole blood (Yang et al., 1999a) and from hematopoietic stem $CD34^+$ cells (Huang et al., 1999).

We recently reported that there are significant differences in the membrane dielectric properties of T- and B-lymphocytes, monocytes, and granulocytes, and suggested that these differences could be exploited to discriminate and separate between these leukocyte subtypes under appropriate dielectrophoretic conditions (Yang et al., 1999b). Here, we report the application of DEP-FFF to the separation of human leukocyte subpopulations. First, we show the differences in the frequency-dependent DEP-FFF responses of T- and B-lymphocytes, monocytes, and granulocytes. Next, we present the DEP-FFF separation of T- or B-lymphocytes from monocytes, T-lymphocytes from granulocytes, and monocytes from granulocytes. A programmable DEP force field has been applied to enhance the separation performance in terms of cell purity and separation speed. Finally, we discuss differences in the density and dielectric properties of these leukocyte subtypes.

MATERIALS AND METHODS

Cell preparation

Major leukocyte subpopulations were purified from buffy bags (Gulf Coast Regional Blood Bank, Houston, TX) as described previously (Yang et al., 1999b). In brief, buffy bag samples were processed using Histopaque (Sigma-Aldrich, Dorset, UK) gradient centrifugation. Purified granulocytes were obtained by lysing erythrocytes in the cell pellet using an ammonium chloride solution (8.26% ammonium chloride/1% potassium bicarbonate/0.037% EDTA tetra sodium). Mononuclear cells collected from the interface were incubated with CD3-, CD19-, or CD14-conjugated magnetic beads (Miltenyi Biotec, Auburn, CA) and processed by superMACS (Miltenyi Biotec) to derive T-, B-lymphocytes, and monocytes. The purified T-, B-lymphocytes, monocytes, and granulocytes were then labeled with fluorescein isothiocyanate (FITC)- or phycoerythrin (PE)-conjugated

monoclonal CD3, CD20, CD14, and CD15 antibodies (Becton Dickinson, San Jose, CA), respectively, and were examined by flow cytometry. All leukocytes were shown to have purity >90%.

Labeled leukocytes were washed once and resuspended at $0.5 - 2 \times 10^6$/ml in 8.5% sucrose/0.3% dextrose (wt/wt) buffer (conductivity 10 mS/m) adjusted with RPMI 1640 medium. For separation studies, two purified leukocyte subtypes were mixed at a 1:1 ratio to achieve a final cell concentration of 2×10^6/ml. For on-line flow cytometry identification of separated leukocyte populations, two-color fluorescence labeling was used. For differential analysis of cells in mixtures, double-label staining was performed using CD3-PE and CD14-FITC for T-lymphocyte and monocyte mixtures, CD20-PE and CD14-FITC for B-lymphocyte and monocyte mixtures, CD3-PE and CD15-FITC for T-lymphocyte and granulocyte mixtures, and CD14-PE and CD15-FITC for monocyte and granulocyte mixtures, respectively.

Separation system setup

The experimental DEP-FFF arrangement was similar to that described previously (Huang et al., 1999). Briefly, eight interdigitated microelectrode arrays (electrode element width/spacing = 50 μm) were glued end-to-end onto a supporting glass plate to form the bottom wall of the separation chamber. A Teflon spacer was cut in the middle to provide a separation channel (H 0.42 × W 25 × L 388 mm) and was sandwiched between the bottom wall and a top glass plate with nylon clamps. An injection valve (Rheodyne Model 7010; Rheodyne, Cotati, CA) equipped with a 50-μl loop was connected to the chamber inlet port. Two PEEK tubings (0.0625-in. OD, 0.020-in. ID, Upchurch Scientific, Oak Harbor, WA) were glued to outlet ports on the top and bottom plates. A lab-built PA05-based power amplifier (Apex Microtechnology, Tucson, AZ) was connected to the electrode arrays to generate a nonuniform electrical field in the chamber.

Individual cells exiting the chamber were analyzed by on-line flow cytometry, and cell elution fractograms were constructed. To allow operation of the DEP-FFF separator at high flow rates (>0.2 ml/min) and to achieve maximum cell concentration at the cytometer, two digital syringe pumps (Daigger, Wheeling, IL) were used to provide continuous flow of carrier medium through the chamber. One pump was operated in the infusion mode and the other in withdrawal mode. Cells exited the chamber bottom through the lower tube and were fed directly to the injection needle of the flow cytometer (BRYTE HS, Bio-Rad, Hercules, CA) for detection. The withdrawal pump connected to the top outlet port was set at 90% of the flow rate of the infusion pump, and withdrew only the cell-free portion of the medium. With this configuration, it is important to ensure that the fluid withdrawal rate is sufficiently low so that no cells elute through the top outlet port. Under typical operating conditions for the cells studied here, about 10% of the infused fluid, corresponding to a height of 80 μm in the parabolic flow profile in the chamber, was eluted to the cytometer. Because the maximum equilibrium height of individual leukocytes was less than 65 μm (measured under the light microscope), no cells had exited through the top outlet port. This was verified experimentally by showing that the number of cells counted by the cytometer was independent of the percentage of eluate flown to the cytometer if that percentage was >7%.

In operation, the DEP-FFF chamber was first loaded with sucrose buffer. Fifty microliters of cell samples were then introduced into the inlet port through the injection valve, as described previously (Wang et al., 1998). A 10-kHz DEP signal (4 V p-p) was applied to the electrodes during sample injection so that cells were levitated in the chamber by DEP forces, which prevented cells from adhering to the chamber bottom surface. After injection, cells were allowed 5 min to sediment to positions sufficiently close to the chamber bottom wall so that DEP forces could be effectively applied. Fluid flow through the chamber was then initiated from the infusion syringe pump at a rate of 2 ml/min. Simultaneously, the withdrawal syringe pump was set to remove cell-free carrier medium from the chamber at a rate equal to 90% of the infusion rate. Cells exited the chamber from the bottom outlet port and were fed into the flow cytometer where they were detected, identified, and counted. Five parameters were measured for each cell: elution time, fluorescence (FITC and PE filter set), and forward and side light scatter.

For characterization of DEP-FFF responses of the leukocyte subpopulations, the DEP signal was changed to various frequencies when the flow started. For DEP-FFF separation, a swept-frequency, instead of a single frequency, was used to maximize the differences in equilibrium levitation heights (and thus the velocities) between the two types. After one cell type was eluted, a 5-kHz DEP signal (4 V p-p) was applied to speed up the elution of all remaining cells.

RESULTS

DEP-FFF responses of the leukocyte subtypes

DEP-FFF responses of T-, B-lymphocytes, monocytes, and granulocytes were studied individually as a function of the frequency of the applied field, and are shown in Fig. 2. Take T-lymphocytes and granulocytes as examples. In the frequency range of 5–40 kHz, T-lymphocytes were eluted from the chamber between 4 and 7 min with peaks at ~4.5 min (Fig. 2 *A*). As the frequency increased to above 40 kHz, the elution fractogram slowly broadened with the peak position shifting to ~8 min at 60 kHz. Granulocytes exhibited elution characteristics similar to those of T-lymphocytes at frequencies below 25 kHz (Fig. 2 *D*). However, at frequencies above 30 kHz, granulocyte response was characterized by a rapid broadening of the elution fractogram and no clear elution peak was observed.

The elution peak times for the four major leukocyte subtypes, as calculated from the elution fractograms (Yang et al., 1999a; Huang et al., 1999), were illustrated in Fig. 3 as a function of the field frequency. While T- and B-lymphocytes had fairly similar DEP-FFF frequency responses, significant differences were observed among lymphocytes, monocytes, and granulocytes at frequencies above 25 kHz. Thus, any two leukocyte subtypes, except T- and B-lymphocytes, should be separable using the DEP-FFF method without recourse to additional methods of cell discrimination.

Separation of human leukocyte subpopulations

Separation of monocytes from T- or B-lymphocytes

Following their introduction into the chamber and before initiation of the fluid flow, mixtures of monocytes and T- or B-lymphocytes were allowed to sediment for 5 min under a 10-kHz DEP-field. After the fluid-flow was commenced, the DEP field frequency was swept repetitively at a 1-s period between 20 and 50 kHz for the monocyte/T-lymphocyte mixtures, and between 20 and 40 kHz for monocyte/B-lymphocyte mixtures. During the swept-frequency period, T- or B-lymphocytes were well levitated and eluted from the chamber, whereas monocytes were levitated only slightly and moved slowly through the chamber. After the 10-min swept-frequency application, the frequency was

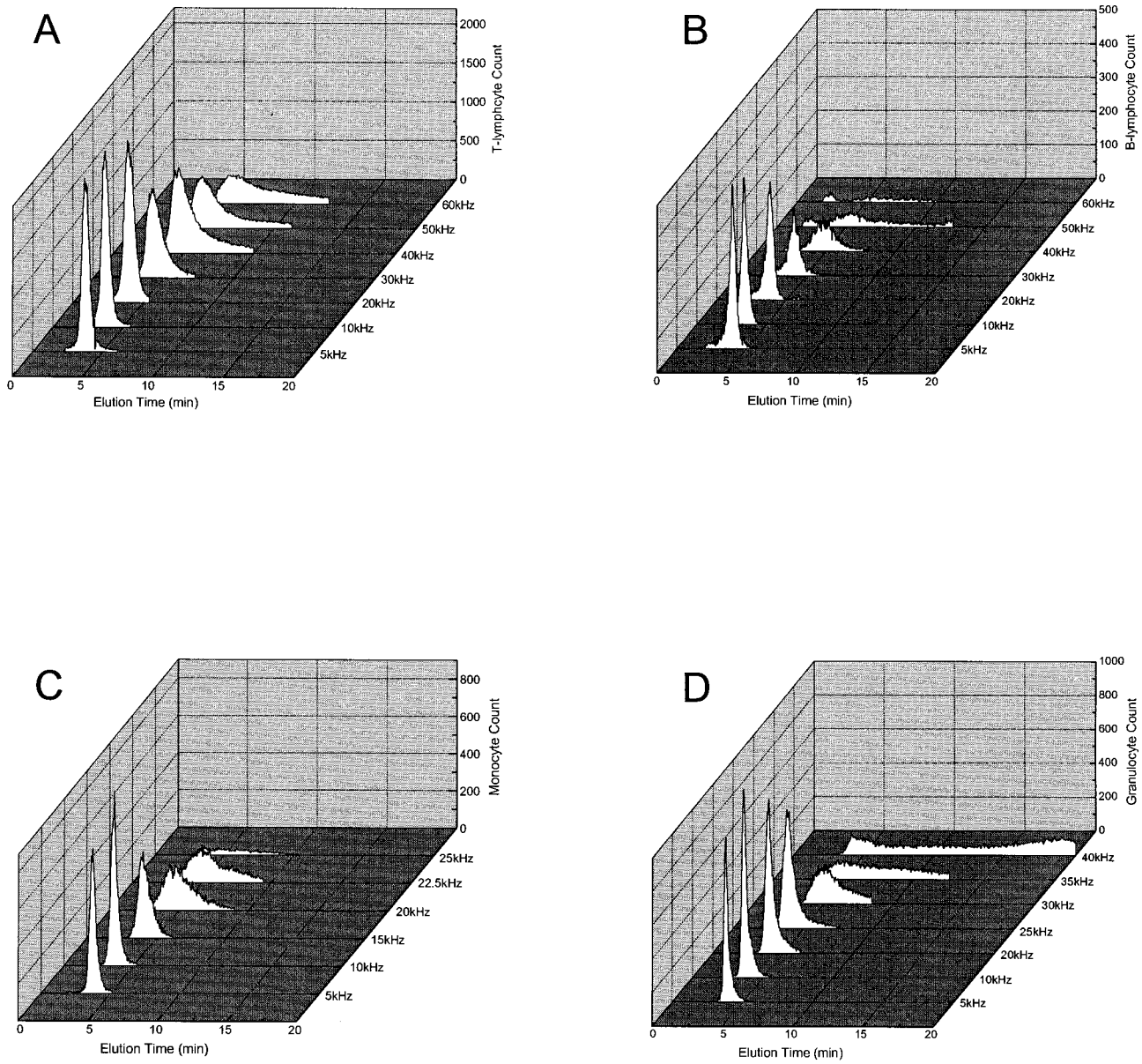

FIGURE 2 DEP-FFF elution fractograms obtained by on-line flow cytometer for (*A*) T-lymphocytes, (*B*) B-lymphocytes, (*C*) monocytes, and (*D*) granulocytes. Cells were suspended at $0.5 - 2 \times 10^6$/ml in an isotonic sucrose/dextrose buffer having an electrical conductivity of 10 mS/m. The applied voltage was 4 V p-p. The infusion and withdrawal syringe pumps were operated at 2 and 1.8 ml/min, respectively.

switched to 5 kHz so that monocytes could be levitated and eluted.

Figure 4 *A* is a typical fractogram depicting the separation of monocytes and T-lymphocytes. It shows that the separation was achieved within 16 min and that the difference in elution peak time between the two cell types was >8 min. Flow cytometry showed that the peak between 4.5 and 5.5 min contained 92% T-lymphocytes whereas the monocyte peak between 12.5 and 13.5 min contained 98% monocytes (Table 1). Similar separation fractograms (not shown) were obtained for monocyte/B-lymphocyte mixtures, and the separation performance is summarized in Table 1.

Figure 4, *B* and *C*, show the contour plots of fluorescence versus exit time for individual cells during the separation of monocytes and T-lymphocytes. Clearly, T-lymphocytes (identified by $CD3^+$-PE) exited the chamber earlier than monocytes (identified by $CD14^+$-FITC).

Separation of granulocytes from T-lymphocytes

For separation of granulocytes from T-lymphocytes, the DEP signal was first swept between 40 and 50 kHz for 8 min, during which time, T-lymphocytes were well levitated and eluted from the chamber. The frequency was then

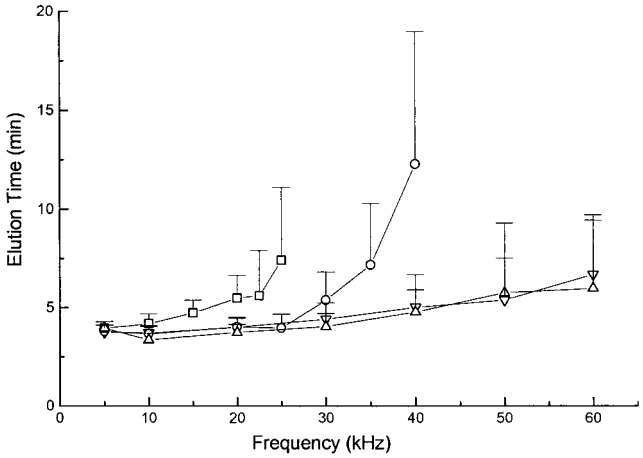

FIGURE 3 Frequency dependency of DEP-FFF elution time for T-lymphocytes (▽), B-lymphocytes (△), monocytes (□), and granulocytes (○). Error bars stand for elution peak width. The elution times and peak widths are calculated from the fractograms in Fig. 2 using the method described previously (Yang et al., 1999a).

switched to 5 kHz to levitate and elute the granulocytes. At the peak elution times for T-lymphocytes (between 5 and 6 min), the eluate contained 87% T-lymphocytes, whereas, at the peak elution time for granulocytes (between 11 and 12 min), the elute contained 94% granulocytes (Fig. 5; Table 1).

Separation of monocytes from granulocytes

Similar procedures to those described above were used for the separation of monocytes from granulocytes, except that a swept frequency between 30 and 35 kHz was applied for 8 min. The DEP-FFF fractogram in Fig. 6 shows that granulocytes eluted from the chamber ahead of monocytes. Separation analysis by flow cytometry revealed that, at the elution peak between 4.5 and 5.5 min, 91% granulocytes were contained in the eluate, whereas, at the peak of 10–11 min, 97% monocytes were contained in the eluate (Table 1).

DISCUSSION

Cell separation mechanics

According to the DEP-FFF theory, the balance of DEP levitation and gravitational forces will equilibrate a cell in the chamber at a height h_{eq} given by

$$h_{eq} = h_0 + A \ln\left(\frac{\mathrm{Re}(f_{CM})}{(\rho_c - \rho_m)g}\right), \quad (1)$$

where A and h_0 are constants that depend on electrode geometry and applied electrical signals (Huang et al., 1997; Wang et al., 1998; Yang et al., 1999a). Cell levitation height is determined by cell density, ρ_c, and dielectric properties, $\mathrm{Re}(f_{CM})$ relative to the carrier medium. Here, $\mathrm{Re}(f_{CM})$ is the

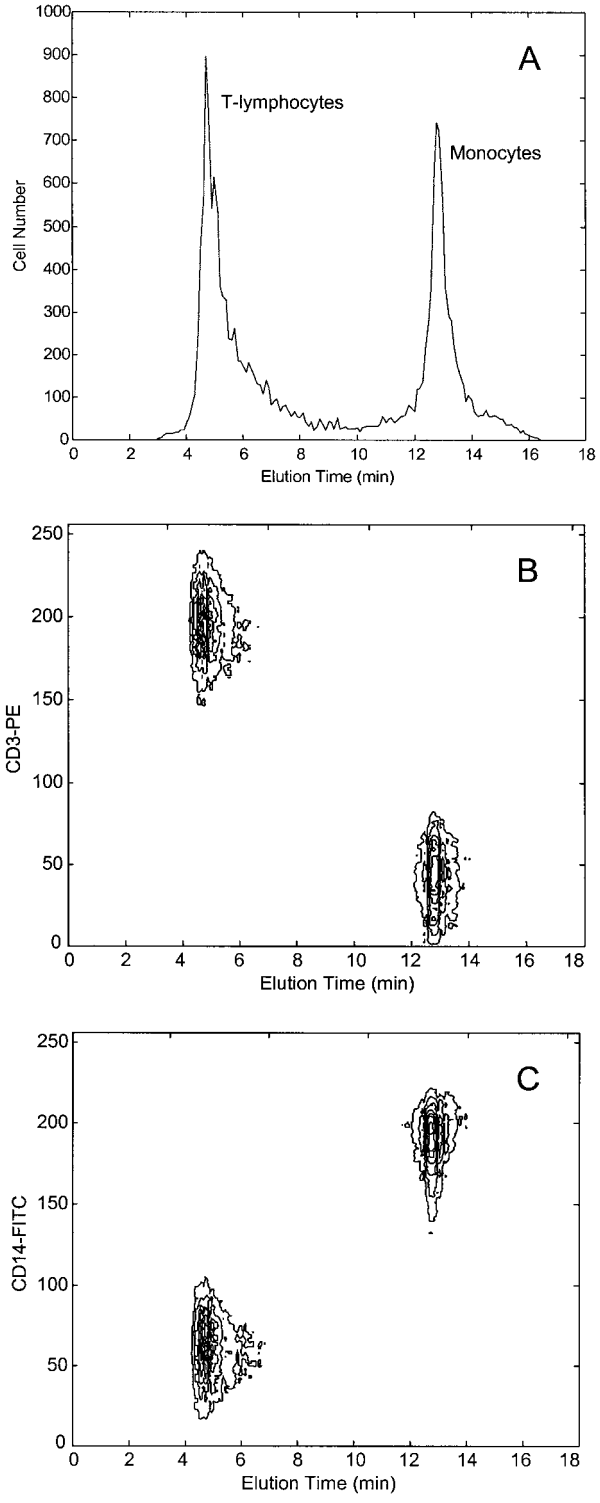

FIGURE 4 (*A*) DEP-FFF fractogram showing the separation of a T-lymphocyte/monocyte mixture. The DEP field was swept for 10 min at frequencies between 20 and 50 kHz, and was then switched to 5 kHz. (*B–C*) The contour plots showing the fluorescence level versus the elution time for cells exiting the DEP-FFF chamber. To facilitate cell identification, T-lymphocytes and monocytes were labeled with PE-conjugated CD3 and FITC-conjugated CD14 antibodies, respectively. Cell suspension, DEP signal voltage, and fluid-flow conditions were the same as in Fig. 2.

real component of the Clausius-Mossotti factor, which is given by $f_{CM} = (\epsilon_c^* - \epsilon_m^*)/(\epsilon_c^* + 2\epsilon_m^*)$, where ϵ_c^* and ϵ_m^* are the frequency-dependent complex dielectric permittivities of the cell and its suspending medium, respectively.

If the chamber width is much greater than the chamber height and flow is fully developed, then a laminar fluid-flow profile will be spontaneously established in the vertical direction within the chamber. A cell at height h_{eq} from the chamber bottom will then be carried along by the flow profile at a velocity V_c and exit the chamber at a time T, given by

$$V_c = 6\langle V_m\rangle \frac{h_{eq}}{H}\left(1 - \frac{h_{eq}}{H}\right), \tag{2}$$

$$T = L/V_c, \tag{3}$$

where H and L are the chamber height and length, respectively, and $\langle V_m\rangle$ is the mean fluid velocity (Huang et al., 1997; Wang et al., 1998; Yang et al., 1999a). Therefore, the cell elution time will be a function of the voltage of the applied DEP field, the electrode geometry, the cell dielectric polarization factor $\mathrm{Re}(f_{CM})$, and the cell density ρ_c. For a specific DEP field condition, cell elution time varies in accordance to $\mathrm{Re}(f_{CM})$ and ρ_c.

Mammalian cells have been typically modeled using single-shell dielectric spheres (Huang et al., 1996; Fuhr et al., 1996; Yang et al., 1999b). In the frequency range operated for DEP-FFF described in this work, $\mathrm{Re}(f_{CM})$ is dominated by cell radius r and membrane (shell) capacitance C_{mem} and can be approximated as

$$\mathrm{Re}(f_{CM}) = \frac{f^2 - f_0^2}{f^2 + 2f_0^2}, \tag{4}$$

$$f_0 = \frac{\sigma_m}{\pi r C_{mem}}, \tag{5}$$

where f_0 is the so-called crossover frequency at which DEP forces acting on the cells are zero, and σ_m is the electrical conductivity of the cell-suspending medium.

We showed in our previous studies that capacitance differences between cells can result from membrane composition or morphological differences. However, because only small permittivity changes are expected to occur through variations in protein/lipid ratio for mammalian cells, membrane area differences associated with morphology are believed to account for most capacitance differences between cells (Sukhorukov et al., 1993; Wang et al., 1994). It follows that cell membrane properties, size, and cell density determine DEP-FFF behavior, and that differences in these parameters form the basis for cell separations in this work.

To analyze the DEP-FFF responses of different leukocyte subtypes, the frequency dependencies of $\mathrm{Re}(f_{CM})$ (Fig. 7) were calculated using Eqs. 4–5 with mean dielectric parameters derived from electrorotation measurements (Yang et al., 1999b). For T-lymphocytes, $\mathrm{Re}(f_{CM})$ varied from -0.5 to -0.15, as frequency increased from 10 to 50 kHz. For monocytes and granulocytes, however, $\mathrm{Re}(f_{CM})$ varied from -0.5 to $+0.15$ and from -0.5 to -0.05, respectively, in a narrow frequency range of 10 to 40 kHz. These results are in agreement with the observation that, with increasing frequency, the elution peaks for granulocytes and monocytes broadened more rapidly than the peaks for lymphocytes. Furthermore, because a certain percentage of the cells experienced positive DEP forces at frequencies above 20 kHz the number of eluted granulocytes and monocytes quickly decreased (Fig. 2). Thus, the variation in DEP-FFF response with frequency is dominated by changes in the dielectric polarization factor $\mathrm{Re}(f_{CM})$.

The differences in $\mathrm{Re}(f_{CM})$ between the four major leukocyte subtypes reflect differences in their size and membrane capacitance (Yang et al., 1999b). As described previously (Yang et al., 1999b), T- and B-lymphocytes have the same average radius of $\sim$3.3 μm and their surfaces are mostly covered by microvilli, although the surfaces of T-lymphocytes appear to be smoother than B-lymphocyte surfaces. In contrast, monocytes and granulocytes are $\sim$1.4 times the size of lymphocytes. Their surfaces commonly possess a great number of folds and ruffles. However, the ruffles on monocytes are flat and wide whereas those on granulocytes are round and narrow. From the T-test results (Table 3 of Yang et al., 1999b) we believe size differences dominated the separation of lymphocytes from monocytes and granulocytes. In contrast, the separation of monocytes and granulocytes depended mostly on differences in the shapes of membrane folds and ruffles and on membrane composition.

Cell size and membrane properties are closely related to cell biological functions. For example, microvilli are generally regarded as a device for increasing the total membrane surface area and thus for facilitating metabolite transport; membrane ruffles have been observed to stretch out to their full heights as cells migrate, and this appear to play a role in facilitating cell motility. Our earlier studies have demonstrated that cell dielectric characteristics are closely associated with cell membrane properties, and that membrane capacitance increases with cell size and cell membrane area associated with membrane-rich morphological features, including microvilli, folds, and ruffles (Wang et al., 1994). Therefore, we expect that cell types that have differences in size or membrane morphology should be separable by DEP-FFF. To predict DEP-FFF separability quantitatively, it is possible to measure the dielectric characteristics of the cell types to be separated by electrorotation measurements, by a DEP-FFF frequency scan, or by dielectric measurements on bulk suspension of pure cells using methods such as time domain spectroscopy. An optimal separation can be found in the frequency range at which the cell populations to be separated demonstrated the largest differences in their DEP-FFF responses.

TABLE 1 Summary of differential analysis of leukocytes by DEP-FFF

Experimental Systems	Cell Types	Purity after Separation* (%)	Separation Time (min)
Monocytes versus T-lymphocytes	Monocytes	98	16
(20–50 kHz, 10 min; 5 kHz, 6 min)†	T-lymphocytes	92	
Monocytes versus B-lymphocytes	Monocytes	94	16
(20–40 kHz, 10 min; 5 kHz, 6 min)†	B-lymphocytes	92	
Granulocytes versus T-lymphocytes	Granulocytes	94	13
(40–50 kHz, 8 min; 5 kHz, 5 min)†	T-lymphocytes	87	
Monocytes versus Granulocytes	Monocytes	97	13
(30–35 kHz, 8 min; 5 kHz, 5 min)†	Granulocytes	91	

*Cell purity after separation was determined by the flow cytometry for the corresponding elution peaks.
†DEP field used for separation consists of a swept frequency segment followed by a fixed frequency.

Unlike gravitational and sedimentation FFF (Yue et al., 1994; Parsons et al., 1996), in which separation performance depends sensitively on cell density, DEP-FFF used cell density through sedimentation forces to act in balance with DEP levitation forces, and cell density is not the only factor that determines separation performance. Take granulocytes and monocytes as an example. Granulocytes have a larger density (1.080–1.085 g/ml) than monocytes (1.058–1.07 g/ml) (Yang et al., 1999b), and would exit the chamber later if both cell types had same Re(f_{CM}) values. However, in our DEP-FFF separation, granulocytes exited earlier than monocytes (Fig. 5). This is because, at 30 kHz, granulocytes, having a mean value of -0.04 for Re(f_{CM}), are levitated by the negative DEP force, whereas monocytes, having a positive mean value of $\sim$0.16, tend to be trapped by positive DEP forces (Yang et al., 1999b).

As reported earlier (Yang et al., 1999b), there is an inherent heterogeneity in each leukocyte subpopulation, and individual cells of one type may possess dielectric properties similar to cells of other types. Such overlapping in cell dielectric distribution may lead to cells of one type being contaminated with other types during DEP-FFF separation. For example, in the separation illustrated in Fig. 5 the T-lymphocyte tail between 7 and 9 min was contaminated with 50% granulocytes.

Separation approaches

To examine separation performance in real time, we used two-color fluorescence staining and on-line flow cytometry to ensure that all the cells in mixtures were identified and counted during the separation. This is an improvement from a previously reported method (Yang et al., 1999a), in which off-line evaluation took additional steps and time. The separation results shown in Table 1 include labeled cells only. Cells other than the components of the binary mixture were excluded by fluorescence gating. It is possible that the CD

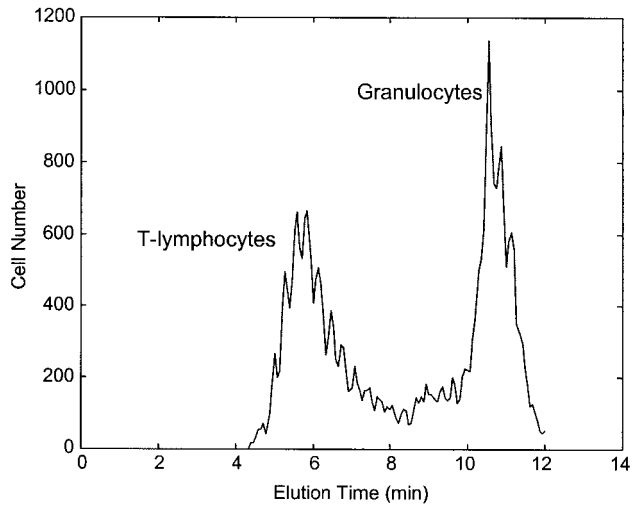

FIGURE 5 DEP-FFF fractogram showing the separation of a T-lymphocyte/granulocyte mixture. The DEP field was swept for 8 min at frequencies between 40 and 50 kHz, and was then switched to 5 kHz. Cell suspension, DEP signal voltage, and fluid-flow conditions were the same as in Fig. 2.

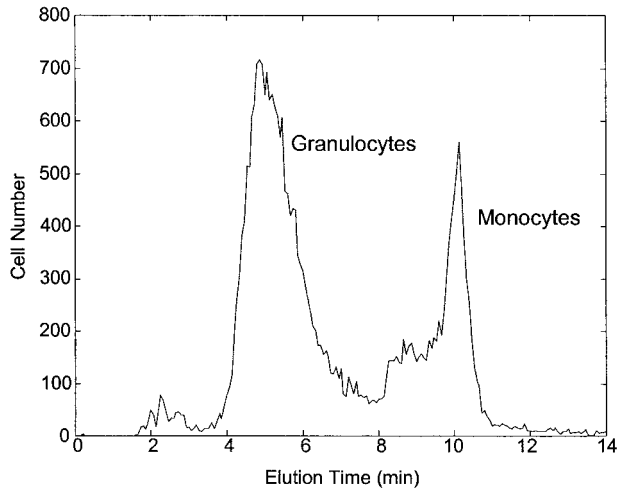

FIGURE 6 DEP-FFF fractogram showing the separation of a monocyte/granulocyte mixture. The DEP field was swept for 8 min at frequencies between 30 and 35 kHz, and was then switched to 5 kHz. Cell suspension, DEP signal voltage, and fluid-flow conditions were the same as in Fig. 2.

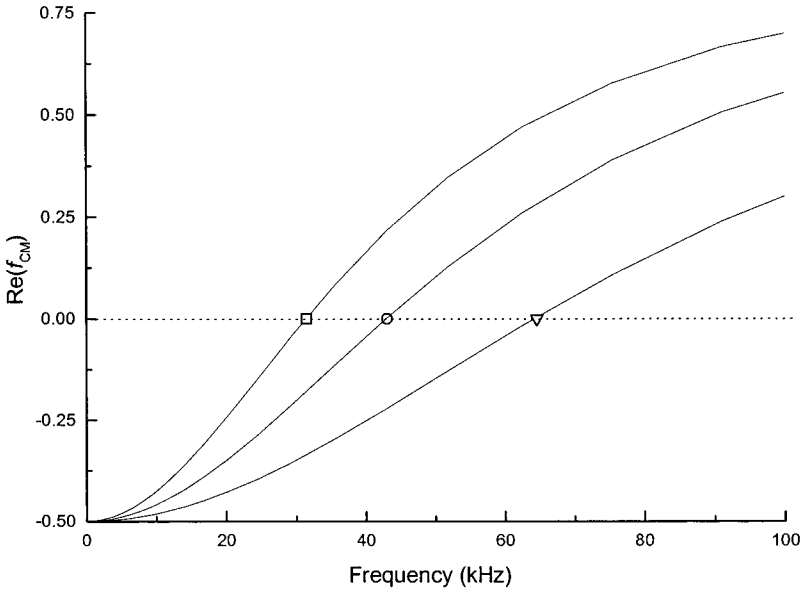

FIGURE 7 The frequency spectra of the dielectric polarization factor Re(f_{CM}) under DEP-FFF separation conditions (conductivity 10 mS/m) for T-lymphocytes (▽), monocytes (□), and granulocytes (○), as calculated using the mean dielectric parameters derived from electrorotation measurements (Yang et al., 1999b).

markers added to the cell surfaces may have changed their membrane dielectric properties. However, in the experiments we conducted, unlabeled cells eluted with a similar profile to CD-labeled cells, suggesting that any such dielectric modifications were not large enough to influence the DEP-FFF properties of the cells studied here.

To achieve efficient cell separation, the goal is to ensure that different cell types experience different time-averaged vertical DEP forces as they traverse the length of the DEP-FFF chamber. The relative DEP forces experienced by different cells are defined by the cellular dielectric differences. However, cells of any given type typically exhibit a somewhat heterogeneous distribution of dielectric properties that can result in a broad elution peak if a single fixed frequency is used and can also result in DEP trapping of some cells. By effectively averaging the DEP forces on cells by applying a field that covers a frequency-band, the swept-frequency approach greatly reduces the number of cells being trapped at the electrodes and causes nearly all cells to be at least slightly levitated. To illustrate this, Fig. 8 shows the calculated elution times for two monocytes as a function of the applied field frequency for both single-frequency and swept-frequency approaches. The two cells are assumed to have a 10% difference in membrane capacitance. At a single frequency of 40 kHz, the monocyte having the larger membrane capacitance is trapped at the electrodes by positive DEP forces, while the other cell is levitated and eluted after 4 min. In contrast, for a swept-frequency signal centered at

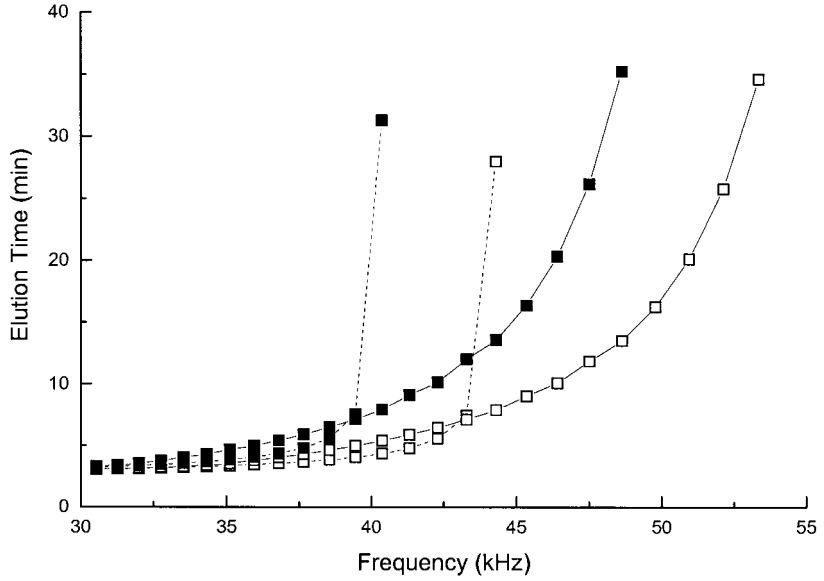

FIGURE 8 Elution times of two monocytes having a 10% difference in membrane capacitance as a function of the DEP-field frequency for both single-frequency (*dotted curves*) and swept-frequency (*solid curves*) methods, as calculated using Eqs. 1–5 with the following parameters. Cell radius $r = 4.63\ \mu$m, membrane capacitance $C_{mem} = 15.3$ (□), 16.8 mF/m^2 (■), cell density $\rho_c = 1.065$ g/ml, medium conductivity $\sigma_m = 10$ mS/m, medium density $\rho_m = 1.033$ g/ml. With a single frequency of 40 kHz, the monocyte having the small capacitance is eluted at 4 min, whereas the other is expected to be trapped at the electrode edges by positive DEP forces. In contrast, for a swept frequency between 30 and 50 kHz, both monocytes would be levitated and eluted at times differing by 3 min.

40 kHz, both monocytes are levitated and are eluted at times that differ by ~3 min. Another effect of the DEP force averaging is that large differences in the spread in elution times for the heterogeneous populations can be condensed to yield a more compact elution profile.

In DEP-FFF, cells are discriminated according to differences in their levitation heights. From Eq 1, we can see that changes in the applied voltage will have broadly similar effects on cells equilibrated at different heights. Thus, although it may alter the shape of the elution profile, a voltage sweep cannot bring any improvement to the DEP-FFF discrimination. For fluid velocity, we observed that increasing fluid flow rate up to several ml/min influenced the elution time, i.e., the higher the flow rate, the quicker the cells were separated. Nevertheless, the relative position of the elution peaks was not altered because no hydrodynamic lift effects played a role in DEP-FFF separations for the conditions used in this study. Therefore, a fluid velocity sweep cannot improve DEP discrimination, either.

The performance of DEP-FFF separation reflects limitations in how tightly cells were initially focused in the flow direction (injection mode, relaxation, etc.) and inherent cell dielectric and density heterogeneities. We anticipate that cell chaining may become a problem that influences separation purity when cell concentrations become too high. Nevertheless, the throughput of batch mode separation for the chamber geometry we used was at least 10^6 cells, based on our experiments. Within that range, no deterioration in DEP-FFF performance was observed.

CONCLUSIONS AND PERSPECTIVE

The four major leukocyte subtypes, namely, T- and B-lymphocytes, monocytes, and granulocytes were separated using DEP-FFF. Cells were separated according to differences in their size, density, and membrane properties. High purity and good separation performance was achieved. This is the first time DEP-FFF has been used to separate cell subtypes.

DEP-FFF conditions were programmed to achieve time-varying DEP forces during separation to increase the discrimination between different cell types. Although it is not necessary to use swept frequencies, by doing so it is possible to selectively control the relative time-averaged DEP forces experienced by cells having different dielectric properties, leading to improved performance of the separator. For different applications, we envisage using different signal programming sequences to attain desired separation performances. Optimal multiple or swept-frequency conditions can either be determined empirically or be predicted by computer simulations using Eqs. 1–5 if cell dielectric properties and desired elution characteristics are known. For example, from the computer simulation results in Fig 7, we can predict that it is possible to separate lymphocytes, monocytes, and granulocytes directly from buffy coats, using, first, a swept frequency between 40 and 50 kHz. Only lymphocytes would be levitated and eluted in this frequency range, whereas monocytes and granulocytes would be barely levitated or gently trapped at the electrodes. Second, after lymphocyte elution, the swept frequency would be lowered to 30–35 kHz to levitate and elute the granulocytes while still barely levitating or trapping monocytes. Finally, the frequency would be set to 5 kHz to strongly levitate monocytes and cause their elution. Such programmability suggests that DEP-FFF separation performance can be tailored to many clinical and research applications.

We are grateful to J. Vykoukal for valuable discussions, to J. Noshari and C. Joyce for laboratory assistance, to T. Anderson for help in constructing the DEP-FFF chamber, and to C. Bonnerup for control software.

This work is supported by a National Institutes of Health grant R01 DK51065-01 from the National Institute of Diabetes and Digestive and Kidney Disease and by a research contract from the Electronics Technology Office of the Defense Advanced Research Program Agency (NRaD Contract N66001-97-C-8608 under DARPA Order E934).

REFERENCES

Abts, H., M. Emmerich, S. Miltenyi, A. Radbruch, and H. Tesch. 1989. CD20 positive human B lymphocytes separated with the magnetic cell sorter (MACS) can be induced to proliferation and antibody secretion in vitro. *J. Immunol. Methods.* 125:19–28.

Ali, F. M. K. 1986. Separation of Human Blood and Bone Marrow Cells. Ch. 3. Wright, IOP Publishing Ltd., Bristol, U.K. 54–85.

Barald, K. F. 1987. *In* Cell Separation—Methods and Selected Applications. T. G. Pretlow and T. P. Pretlow, editors. Ch. 5. Academic Press, New York. 89–102.

Becker, F. F., X.-B. Wang, Y. Huang, R. Pethig, J. Vykoukal, and P. R. C. Gascoyne. 1994. The removal of human leukemia cells from blood using interdigitated microelectrodes. *J. Phys. D: Appl. Phys.* 27:2659–2662.

Becker, F. F., X.-B. Wang, Y. Huang, R. Pethig, J. Vykoukal, and P. R. C. Gascoyne. 1995. Separation of human breast cancer cells from blood by differential dielectric affinity. *Proc. Natl. Acad. Sci. USA.* 92:860–864.

Boyum, A. 1974. Separation of blood leucocytes, granulocytes and lymphocytes. *Tissue Antigens.* 4:269–274.

Cantrell, D. A., J. D. Graves, M. Izquierdo, S. Lucas, and J. Downward. 1992. T lymphocyte activation signals. *Ciba Found. Symp.* 164: 208–218.

Cheng, J., E. L. Sheldon, L. Wu, M. J. Heller, and J. P. O'Connell. 1998a. Isolation of cultured cervical carcinoma cells mixed with peripheral blood cells on a bioelectronic chip. *Anal. Chem.* 70:2321–2326.

Cheng, J., E. L. Sheldon, L. Wu, A. Uribe, L. O. Gerrue, J. Carrino, M. J. Heller, and J. P. O'Connell. 1998b. Preparation and hybridization analysis of DNA/RNA from *E. Coli* on microfabricated bioelectronic chips. *Nat. Biotechnol.* 16:541–546.

Chess, L., and S. F. Schlossman. 1976. *In* In Vitro Methods in Cell Mediated and Tumor Immunity. B. R. Bloom and J. R. David, editors. Academic Press, New York. 255–261.

Couraud, P. O. 1994. Interactions between lymphocytes, macrophages, and central nervous system cells. *J. Leukoc. Biol.* 56:407–415.

Eggleton, P., D. Fisher, and N. Crawford. 1992. Heterogeneity in the circulating neutrophil pool: studies on subpopulations separated by continuous flow electrophoresis. *J. Leukoc. Biol.* 51:617–625.

Fuhr, G., and R. Hagedorn. 1996. *In* Electrical Manipulation of Cells. P. T. Lynch and M. R. Davey, editors. Capman and Hall, New York. 37–66.

Gadeberg, O. V., J. M. Rhodes, and S. O. Larsen. 1979. Isolation of human peripheral blood monocytes: a comparative methodological study. *J. Immunol. Methods.* 31:1–10.

Gascoyne, P. R. C., Y. Huang, R. Pethig, J. Vykoukal, and F. F. Becker. 1992. Dielectrophoretic separation of mammalian cells studied by computerized image analysis. *Meas. Sci. Technol.* 3:439–445.

Gascoyne, P. R. C., X.-B. Wang, Y. Huang, and F. F. Becker. 1997. Dielectrophoretic separation of cancer cells from blood. *IEEE Trans. Ind. Appl. Soc.* 33:670–678.

Huang, Y., X.-B. Wang, F. F. Becker, and P. R. C. Gascoyne. 1996. Membrane changes associated with the temperature-sensitive P85gag-mos-dependent transformation of rat kidney cells as determined by dielectrophoresis and electrorotation. *Biochim. Biophys. Acta.* 1282: 76–84.

Huang, Y., X.-B. Wang, P. R. C. Gascoyne, and F. F. Becker. 1997. Introducing dielectrophoresis as a new force field for field-flow-fractionation. *Biophys. J.* 73:1118–1129.

Huang, Y., J. Yang, X.-B. Wang, F. F. Becker, and P. R. C. Gascoyne. 1999. The removal of human breast cancer cells from hematopoietic CD34+ stem cells by dielectrophoretic field-flow-fractionation. *J. Hematother. Stem Cell Res.* 8:481–490.

Markx, G. H., Y. Huang, X. F. Zhou, and R. Pethig. 1994. Dielectrophoretic characterization and separation of microorganisms. *Microbiology.* 140:585–591.

Markx, G. H., and R. Pethig. 1995. Dielectrophoretic separation of cells: continuous separation. *Biotech. Bioeng.* 45:337–343.

Miltenyi, S., W. Muller, W. Weichel, and A. Radbruch. 1990. High gradient magnetic cell separation with MACS. *Cytometry.* 11:231–238.

NRC report of the Committee of Separation Science and Technology. 1987. Separation and Purification: Critical Needs and Opportunities. National Academy Press, Washington, D.C.

Parsons, R., V. Yue, X. Tong, P. Cardot, A. Bernard, J. P. Andreux, and K. Caldwell. 1996. Comparative study of human red blood cell analysis with three different field-flow fractionation systems. *J. Chromatog.* 686:177–187.

Pethig, R., and D. B. Kell. 1987. The passive electrical properties of biological systems: their significance in physiology, biophysics and biotechnology. *Phys. Med. Biol.* 32:933–970.

Pohl, H. 1978. Dielectrophoresis. Cambridge University Press, Cambridge, U.K.

Semple, J. W., D. Allen, W. Chang, P. Castaldi, and J. Freedman. 1993. Rapid separation of $CD4^+$ and $CD19^+$ lymphocyte populations from human peripheral blood by a magnetic activated cell sorter (MACS). *Cytometry.* 14:955–960.

Smeland, E. B., S. Funderud, H. K. Blomhoff, and T. Egeland. 1992. Isolation and characterization of human hematopoietic progenitor cells: an effective method for positive selection of $CD34^+$ cells. *Leukemia.* 6:845–852.

Stein, R. C., and A. G. Dalgleish. 1994. Immunomodulatory agents: the cytokines. *Eur. J. Cancer.* 30A:400–404.

Stephens, M., M. S. Talary, R. Pethig, A. K. Burnett, and K. I. Mills. 1996. The dielectrophoresis enrichment of CD34+ cells from peripheral blood stem cell harvests. *Bone Marrow Transplant.* 18:777–782.

Stout, R. D. 1993. Macrophage activation by T cells: cognate and non-cognate signals. *Curr. Opin. Immunol.* 5:398–403.

Sukhorukov, V. L., W. M. Arnold, and U. Zimmermann. 1993. Hypotonically induced changes in the plasma membrane of cultured mammalian cells. *J. Membr. Biol.* 132:27–40.

Trinchieri, G., M. Wysocka, A. D'Andrea, M. Rengaraju, M. Aste-Amezaga, M. Kubin, N. M. Valiante, and J. Chehimi. 1992. Natural killer cell stimulatory factor (NKSF) or interleukin-12 is a key regulator of immune response and inflammation. *Prog. Growth Factor Res.* 4:355–368.

van Zaanen, H. C., R. J. Vet, C. M. de Jong, A. E. von dem Borne, and M. H. van Oers. 1995. A simple and sensitive method for determining plasma cell isotype and monoclonality in bone marrow using flow cytometry. *Br. J. Haematol.* 91:55–59.

Wang, X.-B., Y. Huang, J. P. H. Burt, G. H. Markx, and R. Pethig. 1993. Selective dielectrophoretic confinement of bioparticles in potential energy wells. *J. Phys. D: Appl. Phys.* 26:1278–1285.

Wang, X.-B., Y. Huang, P. R. C. Gascoyne, F. F. Becker, R. Hözel, and R. Pethig. 1994. Changes in Friend murine erythroleukaemia cell membranes during induced differentiation determined by ROT. *Biochim. Biophys. Acta.* 1234:185–194.

Wang, X.-B., J. Vykoukal, F. F. Becker, and F. F. Gascoyne. 1998. Separation of polystyrene beads using dielectrophoretic/gravitational field-flow-fractionation. *Biophys. J.* 74:2689–2701.

Yang, J., Y. Huang, X.-B. Wang, F. F. Becker, and P. R. C. Gascoyne. 1999a. Cell separation on microfabricated electrodes using dielectrophoretic/gravitational field-flow-fractionation. *Anal. Chem.* 71: 911–918.

Yang, J., Y. Huang, X. J. Wang, X.-B. Wang, F. F. Becker, and P. R. C. Gascoyne. 1999b. Dielectric properties of human leukocyte subpopulations determined by electrorotation as a cell separation criterion. *Biophys. J.* 76:3307–3314.

Yue, V., R. Kowal, L. Neargarder, L. Bond, A. Muetterties, and R. Parsons. 1994. Miniature field-flow fraction system for analysis of blood cells. *Clin. Chem.* 40:1810–1814.